Optics Communications 284 (2011) 2307–2311

Contents lists available at ScienceDirect

Optics Communications

journal homepage: www.elsevier.com/locate/optcom

The relationship between refractive index-energy gap and the film thickness effect on the characteristic parameters of CdSe thin films

Yunus Akaltun [a], M. Ali Yıldırım [b,*], Aytunç Ateş [c], Muhammet Yıldırım [c]

[a] Department of Electronic and Automation, Vocational Training School, Erzincan University, Erzincan, Turkey
[b] Department of Physics, Science and Art Faculty, Erzincan University, Erzincan, Turkey
[c] Department of Physics, Science Faculty, Atatürk University, Erzurum, Turkey

ARTICLE INFO

Article history:
Received 10 August 2010
Accepted 29 December 2010
Available online 18 January 2011

Keywords:
CdSe
SILAR
Film thickness
Refractive index
Effective mass
Dielectric constant

ABSTRACT

CdSe thin films were deposited on glass substrates using Successive Ionic Layer Adsorption and Reaction (SILAR) method at room temperature and ambient pressure. The relationship between refractive index and energy bandgap was investigated. The film thickness effect on the structural, morphological, optical and electrical properties of CdSe thin films was investigated. The X-ray diffraction (XRD) and scanning electron microscopy (SEM) studies showed that all the films exhibit polycrystalline nature with hexagonal structure and are covered well with glass substrates. The crystalline and surface properties of the films improved with increasing film thickness. The optical absorption studies revealed that the films are found to be a direct allowed transition. The energy bandgap values were changed from 1.93 to 1.87 eV depending on the film thickness. The electron effective mass (m_e^*/m_o), refractive index (n), optical static and high frequency dielectric constant (ε_o, ε_∞) values were calculated by using the energy bandgap values as a function of the film thickness. The resistivity of the films changed between 10^6 and 10^2 Ω-cm with increasing film thickness at room temperature.

© 2011 Elsevier B.V. All rights reserved.

1. Introduction

There has been increasing interest during the past few decades in II–VI group semiconductor compound thin films because of their wide application in various fields of optoelectronic technology. CdSe is a popular material from the II–VI group. It has attracted most attention for various applications such as thin film transistors, sensors, lasers, photoconductors, gamma ray detectors [1–3], and photoelectrochemical cells (PECs) [4]. CdSe is naturally grown as n-type and hexagonal, cubic or mixed (hexagonal-cubic) crystal structures with direct bandgap energy of 1.74 eV at room temperature [3,5,6]. The resistivity values of CdSe thin films may be adjusted between 10^3 and 10^6 Ω-cm by changing the deposition conditions and techniques [3,7–9].

Different chemical methods such as SILAR [7,9], Chemical Bath Deposition (CBD) [1,8], Spray Pyrolysis (SP) [3,10], Electrodeposition [10,11] etc. have been used to obtain CdSe thin films. The SILAR method, introduced by Nicolau [12], is a unique method by which thin films of compound semiconductors can be deposited alternately by means of the dipping substrate into the aqueous solutions of containing ions for each component. The growth of thin films during the SILAR method occurs only heterogeneously on the solid–solution interface due to the intermediate rinsing step between the cation and anion immersions. Therefore, the thickness of the film can easily be controlled by the number of growth cycles used [13,14].

In this paper, CdSe thin films have deposited on glass substrates using SILAR method. The influence of film thickness on the structural, morphological, optical and electrical properties of CdSe thin films has been investigated. Characterization of the films has been done using XRD, SEM, optical absorption measurements and the two-point-probe method.

2. Experimental procedure

In this study, CdSe thin films were deposited on glass substrates using SILAR method at room temperature and ambient pressure. To deposit CdSe thin films, 0.1 M $CdCl_2$ solution at pH 5.5 and 0.13 M Na_2SeSO_3 solution at pH 10.5 were used as cationic and anionic precursor solutions, respectively. The adsorption, reaction and rinsing times were chosen experimentally so that deposition occurred layerwise and resulted in homogeneous thin film structure.

Substrate cleaning plays an important role in the deposition of thin films. The glass substrates were cleaned ultrasonically for 10 min, first in acetone and then in a 1:1 ethanol:water solution. The substrates were dried and stored in desiccators.

To deposit CdSe, one SILAR growth cycle involves the four following steps: 1) immersing the substrate in the $CdCl_2$ solution for 25 s for the adsorption of cadmium ions on the substrate surface; 2) immersing immediately the withdrawn substrates in double distilled

* Corresponding author. Tel.: +90 446 2243097; fax: +90 446 2243016.
E-mail address: mayildirim@erzincan.edu.tr (M.A. Yıldırım).

0030-4018/$ – see front matter © 2011 Elsevier B.V. All rights reserved.
doi:10.1016/j.optcom.2010.12.094

water for 50 s to remove loosely bound species of Cd^{2+} ions; 3) immersing the substrate in the Na_2SeSO_3 solution for 25 s for the selenide ions (Se^{2-}) to react with the preadsorbed Cd^{2+} ions to form a thin layer CdSe and 4) rinsing the substrate again in double distilled water for 50 s separates out the unreacted Se^{2-} ions loosely bound to the CdSe. Thus one SILAR cycle of CdSe deposition was completed. The film thicknesses were calculated to be 255, 320 and 400 nm using the optical interference method.

For investigating the film thickness effect on the characteristic parameter of the films, XRD, SEM, optical absorption measurements and the two-point-probe method were used. For structural studies, a Rigaku 2200D/Max, X-Ray Diffractometer using Cu Kα (λ = 1.5405 Angstrom (Å)) radiation with 2θ of 20–60° was used. Surface morphology was studied using the Zeiss Supra 50 VP model SEM. In order to study the optical properties of the generated films, the absorption measurements were carried out using a Perkin-Elmer UV/VS Lambda 2S Spectrometer with a wavelength resolution better than ±0.3 nm at room temperature. The electrical resistivity of these films was measured using the two-point-probe method in the temperature range of 300–500 K. The contact area on the films was defined (0.2 cm^2) and silver paste was applied to ensure good ohmic contacts.

3. Result and discussion

3.1. Structural analysis

The structural analysis of CdSe thin films was carried out by using XRD varying the diffraction angle, 2θ from 20 to 60°. The XRD patterns of the films are shown in Fig. 1. The XRD patterns of the films indicate the existence of a CdSe single phase with a hexagonal structure. As seen in Fig. 1, all the films have polycrystalline structure with orientation along with different planes. These planes are (002), (101), (110) and (112). We observed that all the films have the same crystal structure but the intensities and full width at half maximum (FWHM) values of these peaks changed with different film thicknesses. The diffraction peak intensities increased with increasing film thickness. These changes may be attributed to the improvement of crystallinity of the films by film thickness. It is seen from Fig. 1 that although some peaks disappeared with changing film thickness, the (002) peak is still dominant peak in all the films. The best crystallinity is seen in 400 nm film thickness. For different film thicknesses, the observed and standard d values, (h,k,l) miller indices, diffraction angle (2θ) of the films were presented in Table 1. The broad hump in the range 2θ = 20–30° is due to the amorphous glass substrate. All of these results are in agreement with relevant literature [3,5,7,15].

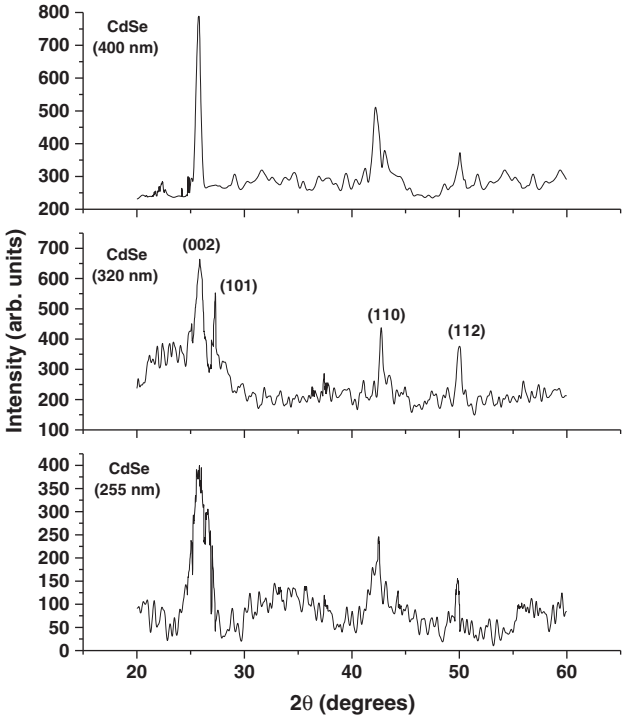


Fig. 1. The XRD patterns of CdSe thin films as a function of film thickness.

The structural parameters such as grain size (D), dislocation density (δ), FWHM (β) for all films were evaluated by XRD patterns and presented in Table 2. The grain size of the thin films was calculated by XRD patterns using Debye Scherrer's formula,

$$D = \frac{0.9\lambda}{\beta \cos\theta} \quad (1)$$

where D is the grain size, λ is the X-ray wavelength used, β is the angular line width at half-maximum intensity in radians and θ is Bragg's angle. We calculated the grain size and dislocation density of the films using the FWHM of (002) peak obtained through the Scherrer's method. Additionally, to have more information on the amount of defects in the films, the dislocation density (δ) was evaluated by the formula [16],

$$\delta = \frac{1}{D^2}. \quad (2)$$

Larger D, smaller β and δ values indicate better crystallization of the films. As can be seen in Fig. 1 and Table 2, the better crystallization turned out to be 400 nm for film thickness in accordance with to the D, β and δ values.

3.2. Surface morphological analysis

It is known that the surface properties of the films influence their optical and electrical properties which are important factors in applications to optoelectronic devices. Thus, it is very important to investigate the surface morphology of the films. Fig. 2 shows the SEM micrograph images of CdSe thin films. It is obvious from Fig. 2a that the 255 nm thickness film does not have a smooth and homogeneous surface morphology with holes and cracks. The uniform, dense, smooth and well-adhered to the substrates of the films increased with increasing film thickness (Fig. 2b–c). Consequently, the surface properties of the CdSe thin films appear to have changed significantly

Table 1
The d values, 2θ and (hkl) miller indices of CdSe thin films as a function of film thickness.

(hkl)	Standard d (Å)	CdSe (255 nm)		CdSe (320 nm)		CdSe (400 nm)	
		2θ (deg.)	d (Å)	2θ (deg.)	d (Å)	2θ (deg.)	d (Å)
(002)	3.517	25.82	3.447	25.84	3.444	25.78	3.453
(101)	3.300	–	–	27.30	3.263	–	–
(110)	2.151	42.50	2.125	42.72	2.114	42.22	2.137
(112)	1.836	49.82	1.828	50.02	1.822	50.04	1.821

Table 2
The grain size (D), dislocation density (δ) and full width at half maximum (FWHM) values of CdSe thin films as a function of film thickness.

	CdSe (255 nm)	CdSe (320 nm)	CdSe (400 nm)
FWHM	1.1828	0.5623	0.4385
D (nm)	6.89	14.49	18.58
$\delta \times 10^{-4}$ (nm^{-2})	210.65	47.62	28.96

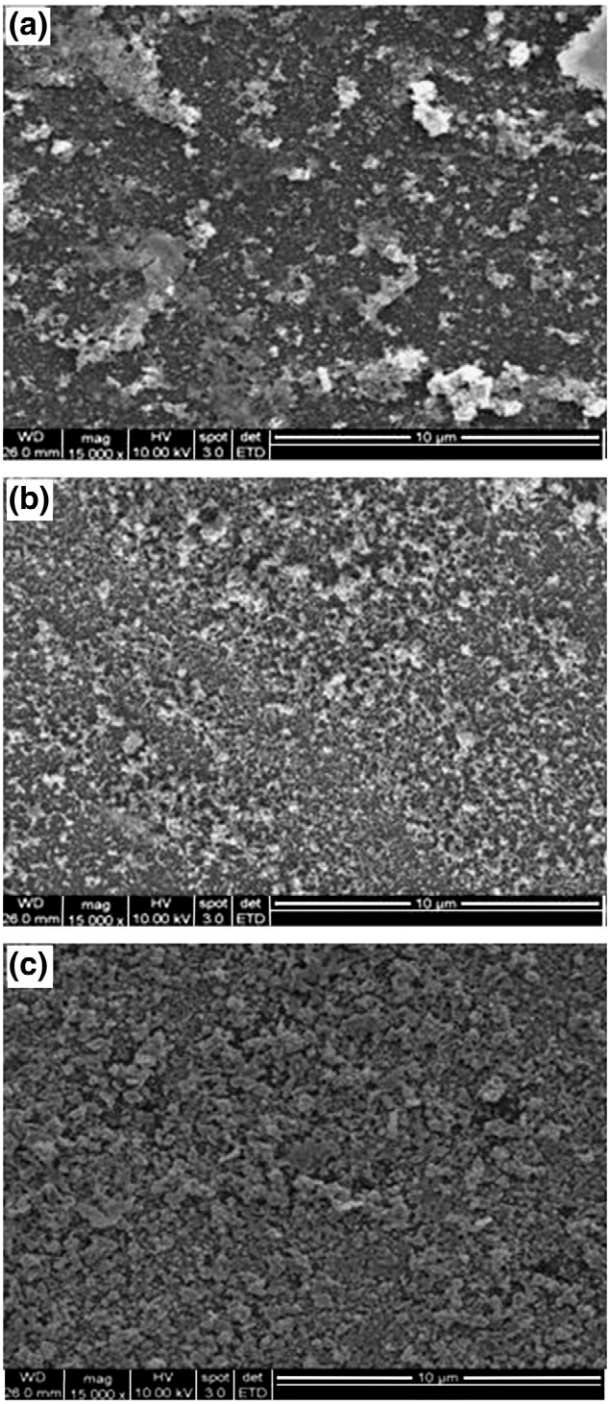


Fig. 2. SEM images of CdSe thin films [255 nm (a), 320 nm (b) and 400 nm (c)] at 15,000× magnification.

with film thickness. Especially, for 400 nm thickness, all of the surface properties are better than the others. These results are in agreement with XRD measurements.

3.3. Optical characterization

Absorption measurements were carried out at room temperature. The energy bandgaps of CdSe films were calculated by using the optical absorption spectra. To determine the energy bandgap values, we plotted $(\alpha h\nu)^2$ versus $(h\nu)$ where α is the absorption coefficient and $h\nu$ is the photon energy. The theory of interband absorption shows that at the edge of optical absorption the absorption coefficient α varies with the photon energy $h\nu$ according to the [14,17],

$$\alpha = \frac{A}{h\nu}\left(h\nu - E_g\right)^n \tag{3}$$

where A is a constant, E_g is the optical bandgap and n assumes values of 1/2, 2, 3/2 and 3 for allowed direct, allowed indirect, forbidden direct and forbidden indirect transitions, respectively. The bandgap energies of the films were determined by the extrapolation of the linear regions on the energy axis $(h\nu)$, as shown in Fig. 3.

The film thickness effect on the absorption measurements was investigated. As can be seen from Fig. 3 and Table 3, the bandgap values decreased from 1.93 to 1.87 eV with increasing film thickness. The decreasing in bandgap with increasing film thickness can be attributed to the improvement in the crystals, in morphological changes of the films, in changes of atomic distances and grain size and structural defects in the films. There is a possibility of structural defects in the films due to their preparation at room temperature; this could give rise to the allowed states near the conduction band in the forbidden region. In case of thick films, these allowed states may as well merge with the conduction band resulting in the reduction of the bandgap. This result is in agreement with literature, XRD and SEM results [7,13,15,18,19].

The refractive index (n), electron effective mass (m_e^*/m_o) and dielectric constant (ε) of semiconducting materials are very important in determining the optical and electrical properties of the crystals. Knowledge of n is essential in the design of heterostructure lasers in optoelectronic devices as well as in solar cell applications. The refractive index of the films was calculated using Moss relation [20,21] that is directly related to the fundamental energy bandgap (E_g),

$$E_g n^4 = k \tag{4}$$

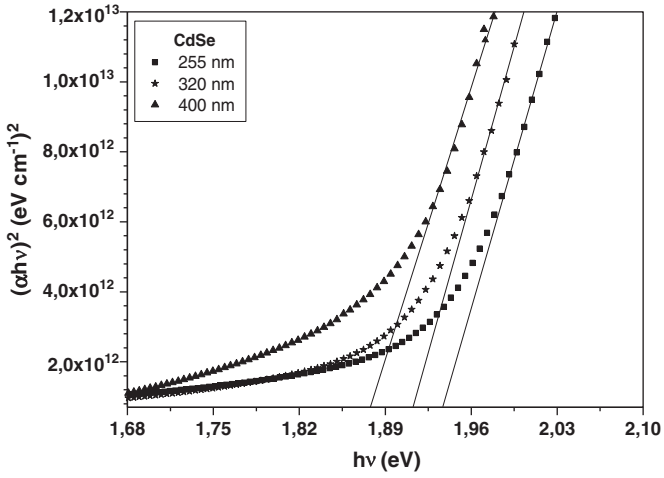


Fig. 3. Plot of $(\alpha h\nu)^2$ versus $h\nu$ for CdSe thin films as a function of film thickness.

Table 3
The bandgap (E_g), conduction band-edge electron effective mass (m_e^*/m_o), refractive index (n), optical static dielectric constant (ε_o) and optical high frequency dielectric constant (ε_∞) values of CdSe thin films as a function of film thickness.

CdSe	E_g (eV)	m_e^*/m_o	ε_o	Moss relation		Ravindra relation	
				n	ε_∞	n	ε_∞
255 nm	1.93	0.156	8.05	2.73	7.45	2.51	6.30
320 nm	1.91	0.153	8.15	2.74	7.51	2.54	6.45
400 nm	1.87	0.149	8.34	2.76	7.62	2.57	6.60

where k is a constant with a value of 108 eV. This relation is preferred to other relations [22] because it is found to give better agreement with the known data for n in II–VI semiconductors [23]. As can be seen from Table 3, the refractive index values increased from 2.73 to 2.76 with increasing film thickness. A different relation between the refractive index and bandgap energy is presented by Ravindra in the following for [21,22],

$$n = 4.16 - 0.85E_g. \tag{5}$$

The dielectric behavior of solids is important for several electron-device properties. Both static and high frequency dielectric constants were evaluated for all the films. The high frequency dielectric constant (ε_∞) was calculated from the following relation [20],

$$\varepsilon_\infty = n^2 \tag{6}$$

where n is refractive index. The static dielectric constant (ε_o) of the films was calculated using a relation expressing the energy bandgap dependence of ε_o for semiconductor compounds in the following form,

$$\varepsilon_o = -33.26876 + 78.61805E_g - 45.70795E_g^2 + 8.32449E_g^3. \tag{7}$$

Similarly to the static dielectric constant, a relation expressing the energy bandgap dependence of the electron effective mass for the semiconductor compounds in the following form,

$$\frac{m_e^*}{m_o} = 5.17004 - 7.46699E_g + 3.63286E_g^2 - 0.57525E_g^3. \tag{8}$$

For different film thicknesses, the calculated n, m_e^*/m_o, ε_∞ and ε_o values of the films were presented in Table 3. All of these results are in agreement with relevant literature [20,24,25].

3.4. Electrical characterization

The measurements of electrical resistivity of the CdSe thin films at different film thicknesses were carried out in the temperature range 300–500 K using the two-point-probe method under dark media. The plots of inverse absolute temperature versus ln ρ are shown in Fig. 4. As can be seen in Fig. 4 and Table 4, the resistivity of the films decreased with increasing in temperature and film thickness which is the indication of typical semiconductor characteristics. The electrical resistivity of the films is in the range between 1.98×10^6 and 2.60×10^2 Ω-cm at room temperature. The reason of the high resistivity can be explained with dislocations and imperfections of the films. The decreasing in resistivity with increasing film thickness can be attributed to the improvement of the crystallization and in morphological changes of the films. As can be seen in Fig. 4, the activation energies were calculated for two linear regions. The activation energy of the films was found to be in the range of 0.37–0.15 eV at low temperature range and 0.41–0.19 eV at high temperature range with increasing film thickness (in Table 4). These results are in agreement with literature [1,7–9].

4. Conclusions

The SILAR method was used to form CdSe thin films on glass substrates at room temperature. The influence of film thickness on the

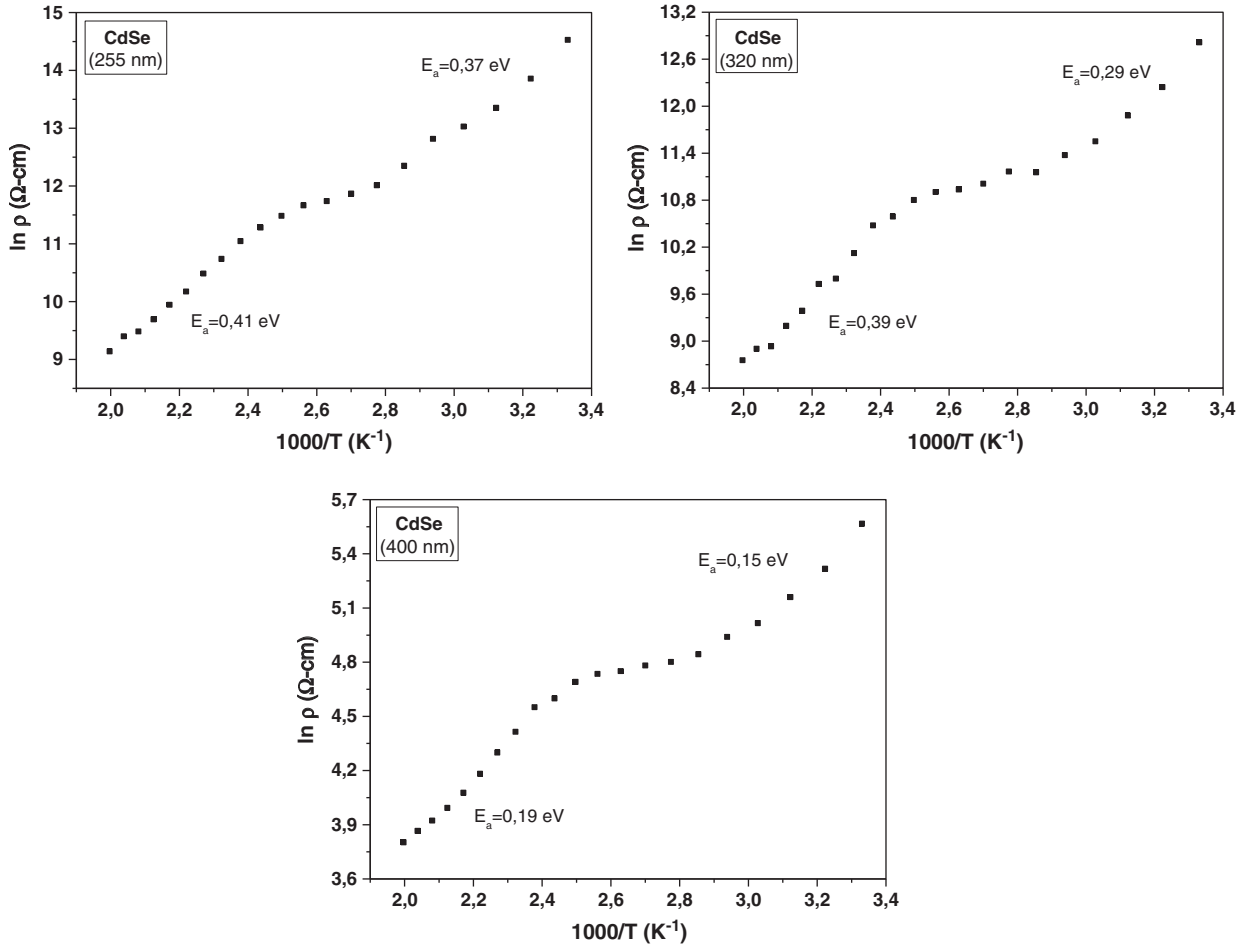


Fig. 4. Plots of log ρ versus (1000/T) for CdSe thin films as a function of film thickness.

Table 4
The resistivity (ρ) and activation energy (E_a) values at different temperatures and film thicknesses for CdSe thin films.

CdSe	ρ (Ω-cm)		E_a (eV)	
	300 K	500 K	LR	HR
255 nm	1.98×10^6	1.09×10^4	0.37	0.41
320 nm	3.63×10^5	6.26×10^3	0.29	0.39
400 nm	2.60×10^2	44.70	0.15	0.19

LR: low temperature region and HR: high temperature region.

structural, morphological, optical and electrical properties of CdSe thin films was studied. The XRD and SEM studies showed that CdSe thin films have a polycrystalline structure and the crystalline and surface properties of these thin films are improved by increasing film thickness. The bandgap values decreased from 1.93 to 1.87 eV and the refractive index (n) of the films increased from 2.73 to 2.76 with increasing film thickness. The resistivity of the films decreased with increasing in temperature and film thickness. The electrical resistivity of the films is in the range between 1.98×10^6 and 2.60×10^2 Ω-cm at room temperature. Consequently, we can say that the film thickness plays an important role on the characteristic parameters of the films and SILAR method is suitable method for depositing CdSe thin films.

References

[1] A.S. Khomane, P.P. Hankare, J. Allays Compd. 489 (2010) 605.
[2] K.C. Sathyalatha, S. Uthanna, P. Jayarama Reddy, Thin Solid Films 174 (1989) 233.
[3] A.A. Yadav, M.A. Barote, E.U. Masumdar, Mater. Chem. Phys. 121 (2010) 53.
[4] U. Farva, C. Park, Sol. Energy Mater. Sol. Cells 94 (2010) 303.
[5] R. Henriquez, P. Grez, E. Munoz, H. Gomez, J.A. Badan, R.E. Marotti, E.A. Dalchiele, Thin Solid Films 518 (2010) 1774.
[6] R.S. Mane, C.D. Lokhande, Thin Solid Films 304 (1997) 56.
[7] H.M. Pathan, B.R. Sankapal, J.D. Desai, C.D. Lokhande, Mater. Chem. Phys. 78 (2002) 11.
[8] S.S. Kale, C.D. Lokhande, Mater. Chem. Phys. 62 (2000) 103.
[9] R.B. Kale, S.D. Sartale, B.K. Chougule, C.D. Lokhande, Semicond. Sci. Technol. 19 (2004) 980.
[10] T. Elango, V. Subramanian, K.R. Murali, Surf. Coat. Technol. 123 (2000) 8.
[11] A.V. Kokate, U.B. Suryavanshi, C.H. Bhosale, Sol. Energy 80 (2006) 156.
[12] Y.F. Nicolau, Appl. Surf. Sci. 22/23 (1985) 1061.
[13] M.Ali Yıldırım, Aytunç Ateş, Opt. Commun. 283 (2010) 1370.
[14] M.Ali Yildirim, Aytunç Ateş, Sens. Actuators A 155 (2009) 272.
[15] D. Pathinettam Padiyan, A. Marikani, K.R. Murali, Mater. Chem. Phys. 78 (2002) 51.
[16] W.D. Callister, Materials Science and Engineering—an Introduction, John Wiley and Sons, New York, 1997.
[17] E. Rosencher, B. Vinter, Optoelectronics, Cambridge University Press, 2002, p. 304.
[18] A. Ateş, M.Ali Yıldırım, M. Kundakcı, A. Astam, Mater. Sci. Semicond. Process. 10 (2007) 281.
[19] V.R. Shinde, C.D. Lokhande, R.S. Mane, Sung-Hwan Han, Appl. Surf. Sci. 245 (2005) 407.
[20] L. Hannachi, N. Bouarissa, Phys. B 404 (2009) 3650.
[21] V.P. Gupta, N.M. Ravindra, Phys. Status Solidi B 100 (1980) 715.
[22] N.M. Ravindra, P. Ganapathy, J. Choi, Infrared Phys. Technol. 50 (2007) 21.
[23] N. Bouarissa, Phys. B 399 (2007) 126.
[24] Y.P. Feng, K.L. Teo, M.F. Li, H.C. Poon, C.K. Ong, J.B. Xia, J. Appl. Phys. 74 (1993) 3948.
[25] D.W. Palmer, <http://www.Semiconductors.CO.UK.> 2008.03.